S factor of the ^{3}H(^{3}H,2n)^{4}He and ^{3}He(^{3}He,2p)^{4}He reactions using a three-cluster exit channel

V. Vasilevsky, A. V. Nesterov, F. Arickx, and J. Broeckhove
Bogolyubov Institute for Theoretical Physics, Kiev, Ukraine
and Universiteit Antwerpen (RUCA), Department of Mathematics and Computer Science, Antwerp, Belgium
(Received 14 July 2000; revised manuscript received 19 January 2001; published 3 May 2001)

The reactions ^{3}H(^{3}H,2n)^{4}He and ^{3}He(^{3}He,2p)^{4}He are investigated within a fully microscopic cluster model featuring a three-cluster exit channel. A hyperspherical harmonics basis is used to describe the three-cluster continuum. The resulting astrophysical S factor of both reactions is in good agreement with experimental data. Analysis of the low-energy scattering parameters reveals no evidence for a hidden resonance state that would increase the cross section of the reactions, and would help to resolve the solar neutrino problem.

DOI: 10.1103/PhysRevC.63.064604 PACS number(s): 24.10.−i, 21.60.Gx, 03.65.Nk, 26.65.+t

I. INTRODUCTION

The problem of the solar neutrino has led to a critical discussion on a number of fundamental principles in modern physics. The problem involves three main aspects: electroweak interactions, nuclear physics, and a model of the sun. In Refs. [1–5] the current status of the solar neutrino problem can be consulted.

The solar energy and the solar neutrino flux are generated by a set of important nuclear reactions. The current status of nuclear astrophysics and some key reactions have been reviewed in Ref. [6]. Those reactions, especially at energy ranges which are typical for the sun, are being intensively studied from both the experimental and theoretical point of view in order to obtain and analyze the cross sections. A major focus of these investigations is the discrepancy between predicted and observed neutrino fluxes.

The reaction ^{3}He(^{3}He,2p)^{4}He contributes for 89% to the pp chain of nuclear synthesis. A specific experimental collaboration (LUNA) was set up to measure this reaction's cross section around the Gamow peak ($\sim$20 keV), the most probable energy at which the reaction occurs in the sun. The progress of the LUNA group was reported in Refs. [7–10]. The cross section has been measured down to the lower edge of the Gamow peak, but there still is a large uncertainty in the cross-section determination and there are important electron screening effects.

The theoretical analysis of the ^{3}He(^{3}He,2p)^{4}He reaction is usually linked to its mirror companion ^{3}H(^{3}H,2n)^{4}He. A comparison of both leads to a better understanding of the underlying dynamics and of the Coulomb effects of reactions with three-cluster exit channels. A first microscopic calculation for these reactions was presented in Ref. [11]. A two-cluster approach was used for both the entrance and exit channels. The nucleon-nucleon fragment cluster (denoted NN for either pp or nn) carried a simple shell-model description, thus featuring a pseudobound state with positive energy. The experimental cross section or S factor at relatively high energy ($\sim$1 MeV) was reproduced by adjusting the Majorana exchange parameter of the effective NN potential. The available experimental data at the (small) energy range relevant in astrophysical reactions were fairly well reproduced. In this model no resonance state appears that would sufficiently amplify the S factor in the appropriate energy range, and thus would constitute an explanation for the solar neutrino problem.

The previous model was further improved or enhanced in Refs. [12–14] by using a more elaborate description of the NN channel, or by simulating the exit channel description using both the $(^4\mathrm{He}+N)+N$ and the $^4\mathrm{He}+(N+N)$ two-cluster configurations. The relative motion of the two clusters was described by a discrete superposition of translated Gaussian functions. In all cases one obtained the same shape for the S factor as a function of energy and there were only limited variations in absolute magnitude.

In this paper we study both the ^{3}H(^{3}H,2n)^{4}He and ^{3}He(^{3}He,2p)^{4}He reactions and use a correct treatment of the corresponding three-cluster exit channels. This will be done in the framework of the microscopic algebraic model (AM) for scattering [15]. A three-cluster version of that model has been introduced in Ref. [16].

The feasibility of the three-cluster AM approach was demonstrated in a calculation of resonance states embedded in the continuum of ^{6}He and ^{6}Be [17]. The energy and width of the 2^+-resonance state in ^{6}He and the 0^+ and 2^+ resonances in ^{6}Be were shown to be in fair agreement with experiment, as shown in Fig. 1 for ^{6}Be. We have also performed a calculation of the bound state energy of ^{6}He in the same model space and have compared it to the results obtained for the three-cluster calculation with the stochastic variational method (SVM) [18,19]. We have used the Minnesota potential without spin-orbit components, and an oscil-

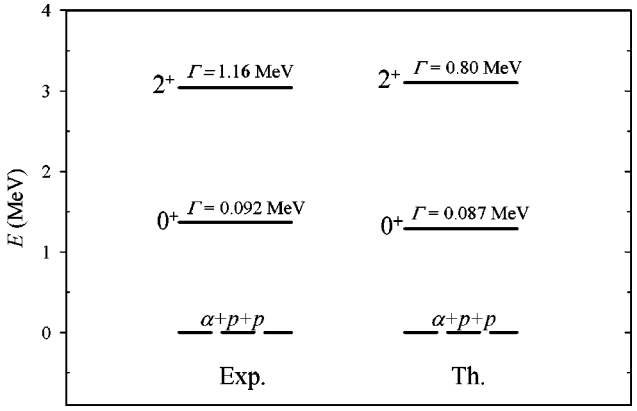

FIG. 1. Energy and width of the 0^+- and 2^+- resonance states in ^{6}Be, calculated in Ref. [17] and compared to experiment (E).

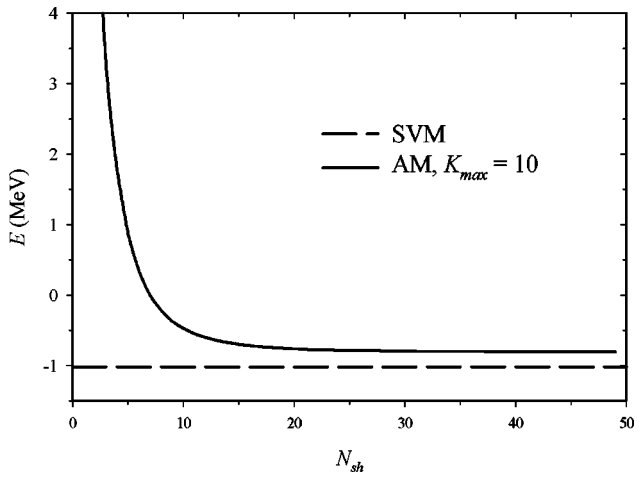

FIG. 2. Ground state of ^{6}He as a function of the number of oscillator shells N in the AM three-cluster model compared to the results of Ref. [19]. The energy is relative to the $\alpha+n+n$ threshold.

lator parameter $b=1.285$ fm which minimizes the α-particle energy as in Ref. [19]. In Fig. 2 we compare our bound-state energy of ^{6}He as a function of number of oscillator shells $N_{\rm sh}$ to the SVM value. We took all hyperspherical harmonics up to $K_{\rm max}=10$ into account, i.e., considered the same basis that was used in Ref. [17]. One notices convergence for $N_{\rm sh}\geqslant 25$ towards $E=-0.8038$ MeV (relative to the $\alpha+n+n$ threshold) within this subspace. This is to be compared to $E=-1.016$ MeV for the full SVM calculation; full convergence towards the SVM result would require additional K values, but this is beyond the scope of this paper. The results reported here have encouraged us to combine the two- and three-cluster AM models to obtain an advanced description of the fusion reactions ^{3}H(^{3}H,2n)^{4}He and ^{3}He(^{3}He,2p)^{4}He.

The organization of the paper is as follows. We first present our description of ^{6}He and ^{6}Be in terms of the relevant two- and three-cluster configurations, and discuss the appropriate boundary conditions. We then elaborate on some aspects of the method. Finally we present the results for the astrophysical S factors of both reactions, discuss the dynamics of the system, and compare with the available experimental data.

II. MODEL SPECIFICS

In the following subsections we will rely heavily on Refs. [11,16] for details concerning the microscopic model. Details concerning the specific cluster configurations used to describe the six-nucleon systems ^{6}He and ^{6}Be can be found in Ref. [17].

A. A combined cluster model

The six-nucleon wave functions will be built up by using both two- and three-cluster configurations, each one fully antisymmetrized:

$$\Psi_L=\mathcal{A}\{\Phi_{3N}\Phi_{3N}\ \ f_L(\mathbf{q}_0)\}+\mathcal{A}\{\Phi_\alpha\Phi_N\Phi_N\ \ g_L(\mathbf{q}_1,\mathbf{q}_2)\}, \tag{1}$$

where the Φ_A (N stands for either nucleon, α for ^{4}He, and $3N$ for ^{3}H or ^{3}He) represent cluster component wave functions, f_L and g_L, respectively, refer to the wave functions of relative motion for the two- and three-cluster system, and $\mathbf{q}_i$ are a choice of Jacobi coordinates describing the configuration of relative position of the clusters.

One of the basic assumptions of the model is [16] that the cluster state is defined by having all its nucleons in a $(0s)$-oscillator wave function. Consequently all of the reaction dynamics, and in particular the behavior of the S-matrix elements is concentrated in the functions describing the relative motion, i.e., f_L and g_L.

The equations for f_L and g_L are cast in the so-called algebraic model (AM) form [16] using an oscillator basis in which to expand the states of relative motion. The appropriate boundary conditions, reflecting the asymptotic behavior of the six-nucleon system, are then expressed in terms of the asymptotic form of the expansion coefficients of f_L and g_L, respectively. This leads to expressions determining the S-matrix elements and cross sections.

A judicious choice has to be made for the Jacobi coordinates $\mathbf{q}$ and for a classification scheme of the wave functions to be used in the expansion of f_L and g_L. We follow the choice made in Ref. [11] for the two-cluster configurations, and the one put forward in Ref. [16] for the three-cluster configuration.

For the two-cluster configuration (in ^{3}H+^{3}H, respectively, ^{3}He+^{3}He) we use spherical coordinates $\mathbf{q}_0=\{q_0,\hat{\mathbf{q}}_0\}$ and take the quantum numbers $\mu=\{n,L,M\}$ to classify the basis states. The n is the familiar radial oscillator quantum number. As we will assume only central components in the nucleon-nucleon interaction, the angular momentum L of relative motion will be an integral of motion for the system.

For the three-cluster configurations (in ^{4}He+p+p, respectively, ^{4}He+n+n) we use hyperspherical coordinates $\{\mathbf{q}_1,\mathbf{q}_2\}=\{\rho,\ \ \Omega\}=\{\rho,\theta,\hat{\mathbf{q}}_1,\hat{\mathbf{q}}_2\}$ with $\rho=\sqrt{\mathbf{q}_1^2+\mathbf{q}_2^2}$, $q_1=\rho\cos\theta$, and $q_2=\rho\sin\theta$. This choice is consistent with a set of quantum numbers $\nu=\{N,K,(l_1l_2)LM\}=\{n_\rho,K,(l_1l_2)LM\}$, in which $N=2n_\rho+K$ represents the total number of oscillator quanta, and n_ρ reflects the number of hyper-radial excitations. K is the hypermomentum, and l_1 and l_2 are the partial angular momenta associated with the choice of Jacobi vectors $\mathbf{q}_1$ and $\mathbf{q}_2$. As discussed in Ref. [16] K is not a good quantum number, and a coupled K-channel calculation, each channel characterized by the set of quantum numbers $\nu_0=\{K,(l_1l_2)LM\}$, has to be performed to solve the dynamical equations. This type of basis is particularly suitable for the so-called Borromean nuclei, and nuclei with pronounced three-cluster features, when the three-cluster threshold represents the prime (lowest energy) decay channel.

B. The boundary conditions

The AM boundary conditions are expressed in terms of the expansion coefficients of the wave functions of relative motion of the cluster configurations. They are directly connected to the boundary conditions in coordinate representa-

tion. For the two-cluster configurations it was shown [16] that the asymptotic form of the expansion coefficients in $f_L = \Sigma c_{n,L}\phi_{n,L}$ can be approximated by

$$c_{n,L} \simeq \sqrt{r_n} f_L(r_n), \tag{2}$$

where the $\{\phi_{n,L}\}$ are oscillator basis functions, and $r_n = b\sqrt{4n+2L+3}$ is the classical turning point of the three-dimensional oscillator with energy $E_n = \hbar\omega(2n+L+3/2)$. In three-cluster configurations the expansion is defined by $g_L = \Sigma d_{n_\rho,L}\phi_{n_\rho,L}$, where the $\{\phi_{n_\rho,L}\}$ now stand for the oscillator basis for three-cluster relative motion. The expansion coefficients behave asymptotically as [16]

$$d_{n_\rho,L} \simeq \rho_n^2 g_L(\rho_n) \tag{3}$$

with $\rho_n = b\sqrt{4n_\rho+2K+6}$. For clarity we have indicated in the preceding discussion only relevant indices. We refer to the original papers for a more elaborate discussion.

In the current study we consider both incoming and outgoing waves for the two-cluster configurations

$$f_L(\mathbf{q}_0) \simeq [\psi_L^{(-)}(k_0 q_0) - S_{\{\mu\},\{\mu\}}\ \psi_L^{(+)}(k_0 q_0)] Y_{LM}(\hat{\mathbf{q}}_0), \tag{4}$$

where $S_{\{\mu\},\{\mu\}}$ is a notation to characterize the elastic two-cluster scattering matrix element for the ^{3}H+^{3}H, ^{3}He $+^3$He channels, respectively, and $Y_{LM}(\hat{\mathbf{q}}_0)$ is the spherical harmonic.

Because we are only interested in reactions with a three-cluster exit-channel, the corresponding asymptotic wave function can be written as [20]

$$g_L(\mathbf{q}_1,\mathbf{q}_2) = g_L(\rho,\Omega) \simeq \sum_{\nu_0} [-S_{\{\mu\},\{\nu_0\}}\ \psi_K^{(+)}(k\rho)] Y_{\nu_0}(\Omega), \tag{5}$$

where $S_{\{\mu\},\{\nu_0\}}$ is the scattering matrix element describing the inelastic coupling between the two- and three-cluster channels, and $Y_{\nu_0}(\Omega)$ being the hyperspherical harmonic [16].

The total cross section is given by the expression

$$\sigma(E) = \frac{\pi}{k_0^2} \sum_{L,S} \frac{(2L+1)(2S+1)}{4} \sum_{\nu_0} |S_{\{\mu\},\{\nu_0\}}|^2 \tag{6}$$

with S the total spin of the six-nucleon system.

As shown in Ref. [20], the asymptotic solutions for incoming and outgoing waves can be written as

$$\psi_{\mathcal{L}}^{(\pm)}(kR) = \frac{1}{\sqrt{k}} W_{\pm i\eta,\lambda}(\pm 2ikR)/R^{(\sigma-1)/2}, \tag{7}$$

where W are the Whittaker functions, and η the Sommerfeld parameter. The parameters $\mathcal{L}$, λ, σ, and η, which differ for two- and three-cluster channels, are summarized in Table I.

By using the aforementioned correspondence between oscillator and coordinate representations, we can now define the boundary conditions for the expansion coefficients

TABLE I. Parameters of the asymptotic solutions (7) for two- and three-cluster channels.

	$\mathcal{L}$	σ	λ	η
Two cluster channel	L	3	$L+\frac{1}{2}$	$\frac{Z_1 Z_2 e^2}{k}\frac{m}{2\hbar^2}\sqrt{\frac{A_1 A_2}{A_1+A_2}}$
Three cluster channel	K	6	$K+2$	$\frac{Z_{eff} e^2}{k}\frac{m}{2\hbar^2}$

$$c_{n,L} \simeq \sqrt{r_n}[\psi_L^{(-)}(k_0 r_n) - S_{\{\mu\},\{\mu\}}\ \psi_L^{(+)}(k_0 r_n)]$$
$$d_{n_\rho,\nu_0} \simeq \rho_n^2[-S_{\{\mu\},\{\nu_0\}}\ \psi_K^{(+)}(k\rho_n)] \tag{8}$$

or, equivalently,

$$c_{n,L} \simeq c_{n,L}^{(-)} - S_{\{\mu\},\{\mu\}}\ c_{n,L}^{(+)}$$
$$d_{n_\rho,\nu_0} \simeq -S_{\{\mu\},\{\nu_0\}}\ d_{n_\rho,\nu_0}^{(+)} \tag{9}$$

using the notations

$$c_{n,L}^{(\pm)} \simeq \sqrt{r_n}\psi_L^{(\pm)}(k_0 r_n)$$
$$d_{n_\rho,\nu_0}^{(\pm)} \simeq \rho_n^2\ \psi_K^{(\pm)}(k\rho_n). \tag{10}$$

The matching of internal and asymptotic regions is equivalent to the one in the traditional resonating group method (RGM). The correspondence between the matching point in coordinate space for RGM and in function space for AM is easily made (see Ref. [16]) through the value of the classical oscillator turning point $r_n = b\sqrt{4n+2L+3}$ for two-cluster systems and $\rho_n = b\sqrt{4n_\rho+2K+6}$ for three-cluster systems. An appropriate value for the matching point can be obtained by choosing sufficiently large values for the total number of oscillator quanta $N = 2n+L = 2n_\rho+K$ in the internal region.

C. Shape analysis

The hyperspherical harmonics could reveal important information on the spatial distribution of clusters, and help to understand the dynamics of the system. This could even reveal possible scenarios for the reactions considered.

These harmonics define a probability distribution in five-dimensional coordinate (momentum) space for fixed values of hyper-radius:

$$dW_{\nu_0}^5(\Omega) = |Y_{\nu_0}(\Omega)|^2 d\Omega,\ \ dW_{\nu_0}^5(\Omega_k) = |Y_{\nu_0}(\Omega_k)|^2 d\Omega_k. \tag{11}$$

By analyzing the probability distribution, one can retrieve the most probable shape of three-cluster configuration or ''triangle'' of clusters. As the full analysis of a function of five variables is nontrivial, one usually restricts oneself to some specific variable(s). In this respect, integrating the

probability distribution $dW^5_{\nu_0}(\Omega)$ over the unit vectors $\hat{\mathbf{q}}_1, \hat{\mathbf{q}}_2$ $(\hat{\mathbf{k}}_1, \hat{\mathbf{k}}_2)$

$$dW_{\nu_0}(\theta) = \int |Y_{\nu_0}(\Omega)|^2 \cos^2\theta \sin^2\theta d\theta \; d\hat{\mathbf{q}}_1 d\hat{\mathbf{q}}_2,$$

$$dW_{\nu_0}(\theta_k) = \int |Y_{\nu_0}(\Omega_k)|^2 \cos^2\theta_k \sin^2\theta_k d\theta_k \; d\hat{\mathbf{k}}_1 d\hat{\mathbf{k}}_2 \tag{12}$$

and introducing the (new) variable(s)

$$\mathcal{E} = \frac{q_1^2}{\rho^2} = \cos^2\theta, \quad \mathcal{E} = \frac{k_1^2}{k^2} = \cos^2\theta_k$$

which, in coordinate space, can be interpreted as the squared distance between the selected pair of clusters or, in momentum space, the relative energy of that pair of clusters, we obtain

$$\begin{aligned} W_{\nu_0}(\mathcal{E}) &= \frac{dW_{\nu_0}(\theta)}{d\theta} \\ &= |N_K^{(l_1,l_2)} \cos^{l_1}\theta \sin^{l_2}\theta P_n^{(l_2+1/2, l_1+1/2)}(\cos 2\theta)|^2 \\ &\quad \times \cos^2\theta \sin^2\theta \\ &= |N_K^{(l_1,l_2)} (\mathcal{E})^{l_1/2} (1-\mathcal{E})^{l_2/2} P_n^{(l_2+1/2, l_1+1/2)}(2\mathcal{E}-1)|^2 \\ &\quad \times \sqrt{\mathcal{E}(1-\mathcal{E})}. \end{aligned} \tag{13}$$

This function represents the probability distribution for relative distance between two selected clusters, respectively, for the energy of relative motion of two selected clusters. The kinematical factor $\cos^2\theta \sin^2\theta$ was included to make $W_{\nu_0}(\mathcal{E})$ proportional to the differential cross section in momentum space, provided the exit channel is described by the single hyperspherical harmonic $Y_{\nu_0}(\Omega)$.

In Fig. 3 we display $W_{\nu_0}(\mathcal{E})$ for some hyperspherical harmonics involved in our calculations. These figures show that different hyperspherical harmonics account for different possible shapes of the three-cluster systems. For instance, the hyperspherical harmonic with $K=10$ and $l_1=l_2=0$ prefers the two selected clusters to move with very small or very large relative energy, or, in coordinate space, prefers them to be close to each other, or far apart. If one or few contributions appear dominantly in the final results, one could obtain a fair idea of the disintegration shape for the three-cluster exit channel.

III. RESULTS

We use the Volkov *NN* interaction [21] in our calculations. It was shown in Refs. [17,22,23] that it provides an acceptable description for the bound state of ^{6}He, as well as for the low energy range in the three-cluster continuum of ^{6}He and ^{6}Be. The Majorana exchange parameter m was set to be 0.54 which is comparable to the one used in Ref. [13]. The oscillator radius was set to $b=1.37$ fm (as in Refs. [17,23]) to optimize the ground state energy of the α particle.

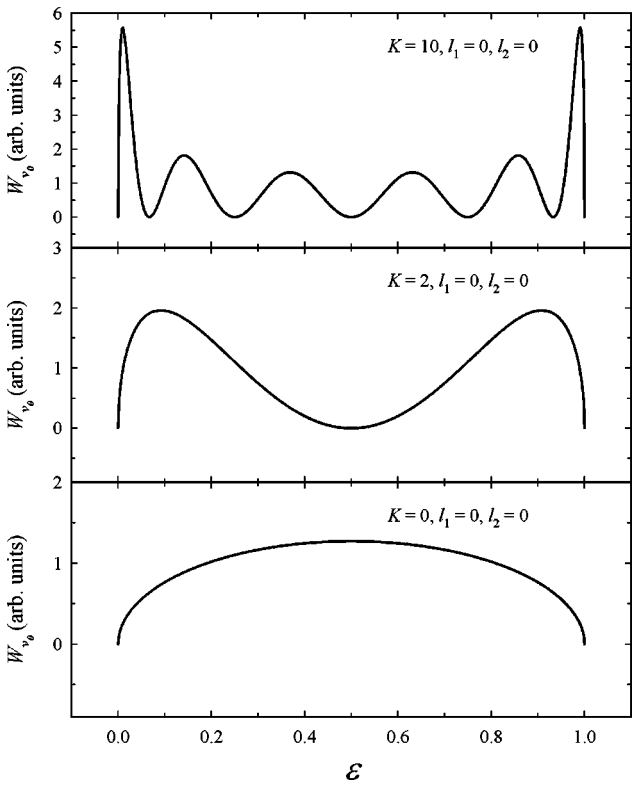

FIG. 3. Function $W_{\nu_0}(\mathcal{E})$ for $K=0$, 2, and 10 and $l_1=l_2=0$.

We should stress that our method (AM) is best suited for an *NN* potential with a relatively soft core, and less appropriate (but also applicable) to *NN* interactions with strong repulsion at short distances between nucleons. This is one of the main reasons for choice of the current *NN* potential.

The Volkov potential does not contain spin-orbital or tensor components so that total angular momentum L and total spin S are good quantum numbers. Moreover, due to the specific features of the potential, the binary channel is uncoupled from the three-cluster channel when the total spin S equals 1; this means that odd parity states $L^\pi = 1^-, 2^-, \ldots$, will not contribute to the reactions.

To describe the continuum of the three-cluster configurations we considered all hyperspherical harmonics with $K \leqslant K_{\max}=10$. In Table II we enumerate all contributing K channels for $L=0$. For each two- and three-cluster channel we used the same number $n=n_\rho=N_{\rm int}$ of basis functions to describe the internal part of the wave function Ψ_L. $N_{\rm int}$ then also defines the matching point between the internal and asymptotic part of the wave function. We used $N_{\rm int}$ as a variational parameter and varied it between 20 and 75, which

TABLE II. Enumeration of all hyperspherical harmonics for total angular momentum $L=0$.

$N_{\rm ch}$	1	2	3	4	5	6	7	8	9	10	11	12
K	0	2	4	4	6	6	8	8	8	10	10	10
$l_1=l_2$	0	0	0	2	0	2	0	2	4	0	2	4

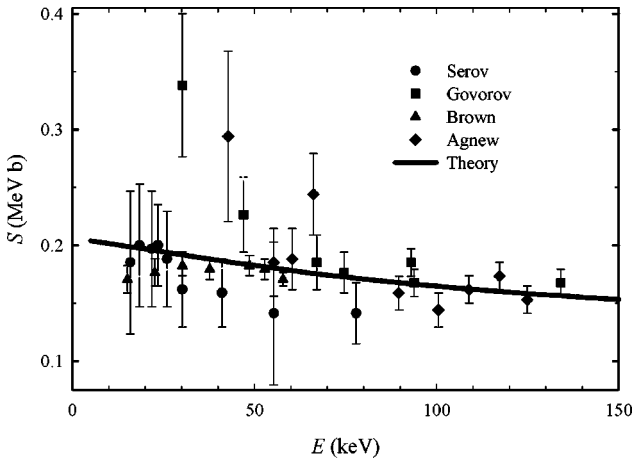

FIG. 4. S factor of the reaction ^{3}H(^{3}H,2n)^{4}He. The experimental data are taken from [26] (Serov), [27] (Govorov), [28] (Brown), and [29] (Agnew).

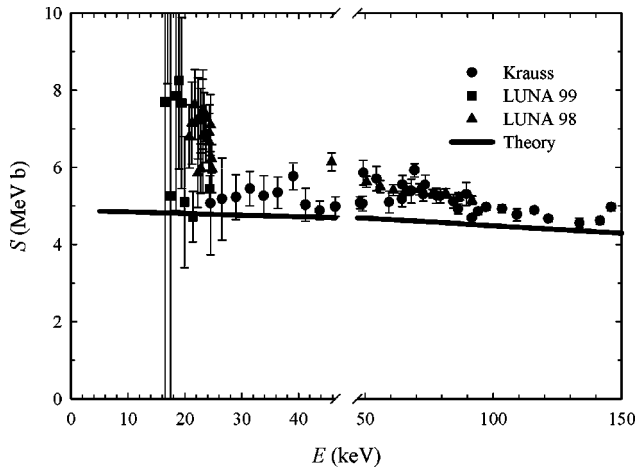

FIG. 5. S factor of the reaction ^{3}He(^{3}He,2p)^{4}He. The experimental data are from Refs. [30] (Krauss), [9] (LUNA 99), and [7] (LUNA 98).

corresponds to a variation in coordinate space of the RGM matching radius approximately between 14 and 25 fm. This variation showed only small changes in the S-matrix elements, of the order of one percent or less, and do not influence any of the physical conclusions. We have then used $N_{\rm int}=25$ for the final calculations as a compromise between convergence and computational effort. We also checked the impact of $N_{\rm int}$ on the unitarity conditions of the S matrix, for instance the relation

$$|S_{\{\mu\},\{\mu\}}|^2+\sum_{\nu_0}|S_{\{\mu\},\{\nu_0\}}|^2=1.$$

We have established that from $N_{\rm int}=15$ on this unitarity requirement is satisfied with a precision of one percent or better. In our calculations, with $N_{\rm int}=25$, unitarity was never a problem. It should be noted that our results concerning the convergence for the three-cluster system with a restricted basis of oscillator functions agree with those of Papp *et al.* [24], where a different type of square-integrable functions was used for three-cluster Coulombic systems.

In Fig. 4 we show the total S factor for the reaction ^{3}H(^{3}H,2n)^{4}He in the energy range $0\leqslant E\leqslant 200$ keV. One notices that the theoretical curve is very close to the experimental data. The total S factor for the reaction ^{3}He(^{3}He,2p)^{4}He is displayed in Fig. 5. It is also close to the available experimental data. The S factor for both reactions is seen to be a monotonic function of energy, and does not manifest any irregularities to be ascribed to a hidden resonance. Thus no indications are found towards explaining the solar neutrino problem.

The astrophysical S factor at small energy is usually written as

$$S(E)=S_0+S_0'E+\frac{1}{2}S_0''E^2. \tag{14}$$

We have fitted the calculated S factor to this formula in the energy range $0\leqslant E\leqslant 200$ keV. For the reaction ^{3}H(^{3}H,2n)^{4}He we obtain the approximate expression

$$S(E)=206.51-0.53\ E+0.001\ E^2\ \text{keV b} \tag{15}$$

and for ^{3}He(^{3}He,2p)^{4}He we find

$$S(E)=4.89-3.99\ E+2.3\quad 10^{-4}\ E^2\ \text{MeV b}. \tag{16}$$

One notices significant differences in the S factor for the ^{6}He and ^{6}Be systems. The NN interaction induces the same coupling between the clusters of entrance and exit channels for both ^{6}He and ^{6}Be. It is the Coulomb interaction that distinguishes both systems, and accounts for the pronounced differences in the cross sections and S factors.

We compare the calculated S factor to fits of experimental results for the reaction ^{3}He(^{3}He,2p)^{4}He:

$$S(E)=5.2-2.8\ E+1.2\ E^2\ \text{MeV b [25]},$$

$$S(E)=(5.40\pm 0.05)-(4.1\pm 0.5)E+(2.3\pm 0.5)E^2\ \text{MeV b [8]},$$

$$S(E)=(5.32\pm 0.08)-(3.7\pm 0.6)E+(1.95\pm 0.5)E^2\ \text{MeV b [10]}. \tag{17}$$

The constant and linear terms of the fit display a good agreement. The difference in energy ranges between the calculated ($0\leqslant E\leqslant 200$ keV) and experimental ($0\leqslant E\leqslant 1000$ keV) fits make it difficult to attribute any significant interpretation to the discrepancy in the quadratic term.

The hyperspherical harmonics method now allows us to study some details of the dynamics of the reactions considered. In Figs. 6 and 7 we show the different three-cluster K-channel contributions (W_{ν_0}) to the total S factor of the reactions. In Fig. 6 these contributions (in % with respect to the total S factor) are displayed for some fixed energy (1 keV), while Fig. 7 shows the dependency of W_{ν_0} (in absolute value) on the energy of the entrance channel. One notices that three hyperspherical harmonics dominate the full result, namely, the $\{K=0;l_1=l_2=0\}$, $\{K=2;l_1=l_2=0\}$ and $\{K=4;l_1=l_2=2\}$, and this is true in both reactions. The con-

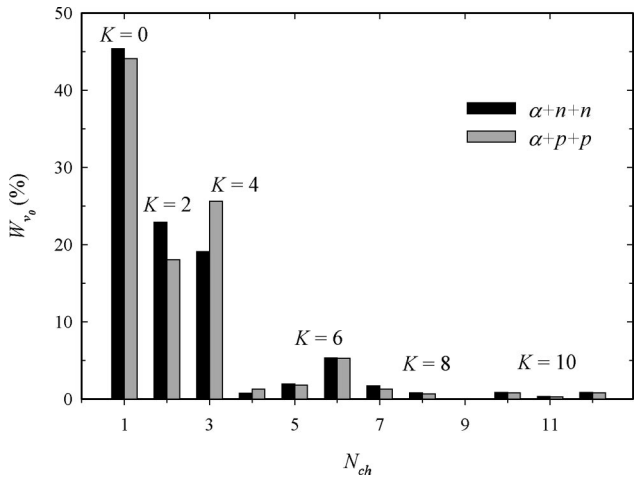

FIG. 6. Contribution of three-cluster channels to the total S factor of the reactions ^{3}H(^{3}H,2n)^{4}He and ^{3}He(^{3}He,2p)^{4}He in a full calculation with $K_{\max}=10$.

tribution of these states to the S factor is more than 95%. There also is a small difference between the reactions ^{3}H(^{3}H,2n)^{4}He and ^{3}He(^{3}He,2p)^{4}He, which is completely due to the Coulomb interaction.

Figures 6 and 7 yield an impression on the convergence of the results and whether the chosen set of hyperspherical harmonics is sufficiently comprehensive. We notice that the contribution of the hyperspherical harmonics with $K>6$ is small compared to the dominant ones. This is true for very small energies as well as for a relatively large energy range ($200\leqslant E\leqslant 1000$ keV). This is corroborated in Fig. 8 where we show the rate of convergence of the S factor in calculations with $K_{\max}$ ranging from 0 up to 10. Our full $K_{\max}=10$ basis is seen to be sufficiently extensive to account for the proper rearrangement of two-cluster configurations into a three-cluster one, as the differences between results becomes increasingly smaller.

To emphasize the importance for a correct three-cluster exit-channel description, we compare the present calculations to those in Ref. [11], where only two-cluster configurations ^{4}He$+2n$, respectively, ^{4}He$+2p$ were used to model the exit channels. In both calculations we used the same interaction and value for the oscillator radius. In Fig. 9 we compare both results for ^{3}H(^{3}H,2n)^{4}He. An analogous picture is obtained for the reaction ^{3}He(^{3}He,2p)^{4}He.

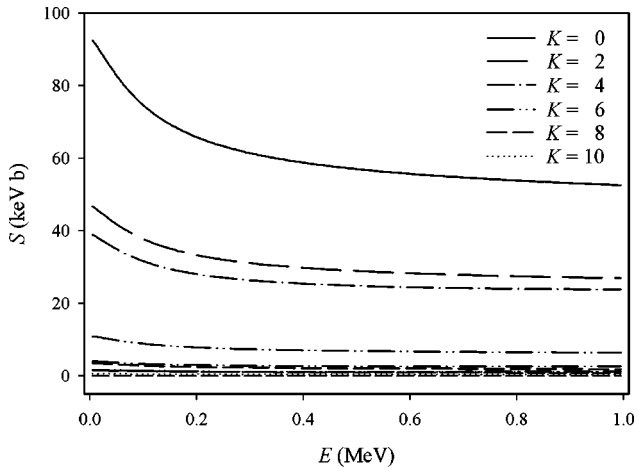

FIG. 7. Contribution of three-cluster channels to the total S factor of the reactions ^{3}H(^{3}H,2n)^{4}He in a full calculation with $K_{\max}=10$ in the energy range $0\leqslant E\leqslant 1000$ keV.

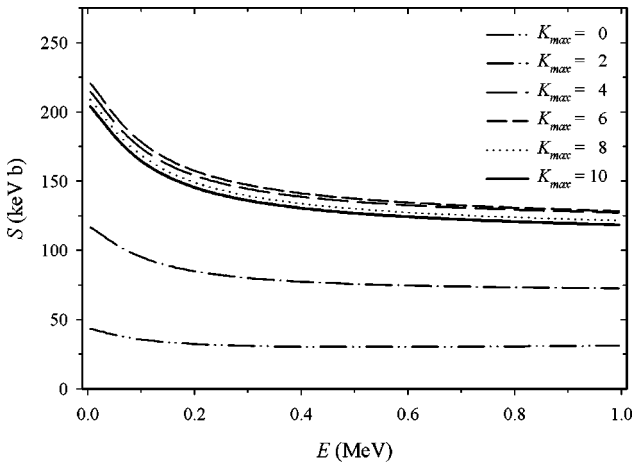

FIG. 8. Convergence of the S factor of the reaction ^{3}H(^{3}H,2n)^{4}He for $K_{\max}$ ranging from 0 to 10.

IV. CROSS SECTIONS

Having calculated the matrix elements of the S matrix by solving the AM equations, we can now easily obtain the total and differential cross sections. In this section we will calculate and analyze onefold differential cross sections, which define the probability for a selected pair of clusters to be detected with a fixed energy E_{12}. To do so we shall consider a specific choice of Jacobi coordinates in which the first Jacobi vector $\mathbf{q}_1$ is connected to the distance between these clusters, and the modulus of vector $\mathbf{k}_1$ is the square root of relative energy E_{12}. With this definition of variables, the cross section is

$$d\sigma(E_{12})\sim\frac{1}{E}\int d\hat{\mathbf{k}}_1 d\hat{\mathbf{k}}_2\left|\sum_{\nu_0} S_{\{\mu\}\{\nu_0\}}Y_{\nu_0}(\Omega_k)\right|^2 \times\sin^2\theta_k\cos^2\theta_k d\theta_k. \tag{18}$$

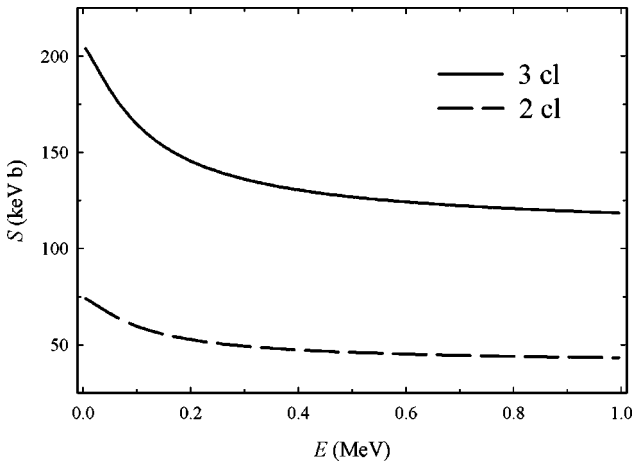

FIG. 9. Comparison of the S factor of the reaction ^{3}H(^{3}H,2n)^{4}He in a calculation with a three-cluster exit-channel and a pure two-cluster model.

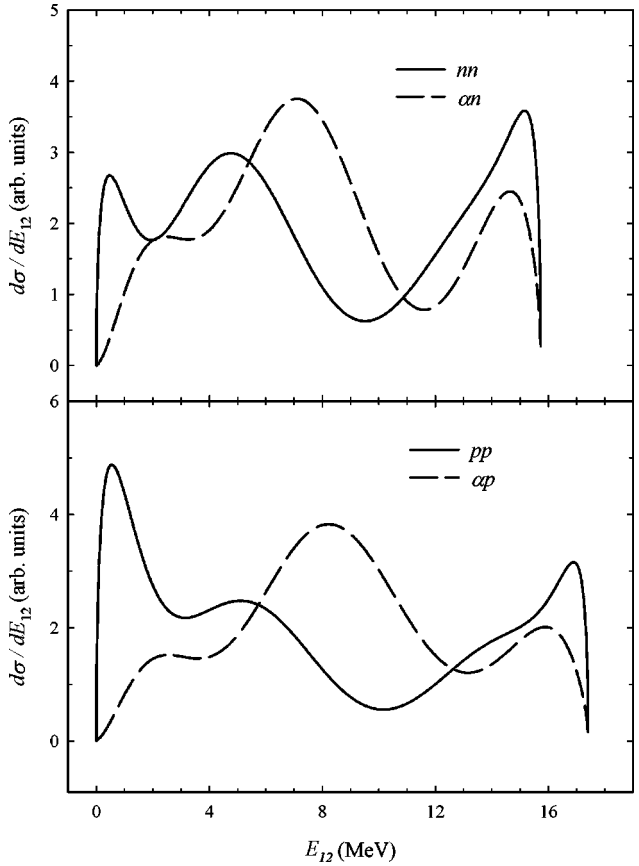

FIG. 10. Partial differential cross sections of the reactions ^{3}H(^{3}H,2n)^{4}He and ^{3}He(^{3}He,2p)^{4}He.

After integration over the unit vectors and substitution of $\sin\theta_k$, $\cos\theta_k$, $d\theta_k$ with

$$\cos\theta_k = \sqrt{\frac{E_{12}}{E}};\quad \sin\theta_k = \sqrt{\frac{E-E_{12}}{E}}$$

$$d\theta_k = \frac{1}{2}\,\frac{1}{\sqrt{(E-E_{12})E_{12}}}\,dE_{12} \tag{19}$$

one can easily obtain $d\sigma(E_{12})/dE_{12}$.

In Fig. 10 we display the partial differential cross sections of the reactions ^{3}H(^{3}H,2n)^{4}He and ^{3}He(^{3}He,2p)^{4}He for the energy $E=10$ keV in the entrance channel. The solid lines correspond to the case when two neutrons (protons) are detected with relative energy E_{12}, while the dashed lines represent the cross sections when the α particle and one of the neutrons (protons) are observed with relative energy E_{12}.

We wish to emphasize the ''measurement'' in which two neutrons or two protons are simultaneously detected. One indeed notices a pronounced peak in the cross section around $E_{12}\simeq 0.5$ MeV. This peak is even more pronounced for the reaction ^{3}He(^{3}He,2p)^{4}He. It means that at such energy two neutrons or two protons could be detected simultaneously with large probability. We believe that this peak can explain the relative success of a two-cluster description for the exit channels. The pseudobound states of nn or pp subsystems

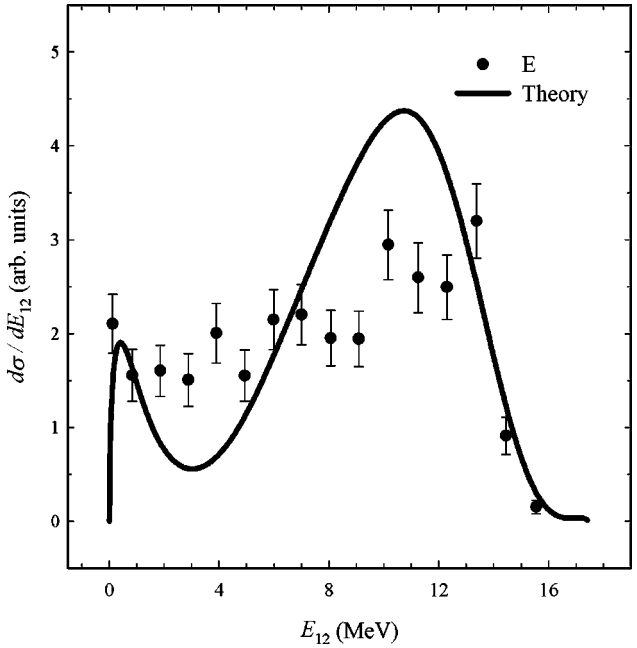

FIG. 11. Calculated and experimental differential cross section for the reaction ^{3}He(^{3}He,2p)^{4}He. Experimental data are taken from Ref. [25].

used in this type of calculations indeed allowed one to obtain a reasonable shape for the astrophysical *S* factor.

Special attention should be paid to the energy range 1–3 MeV in the ^{4}He+n and ^{4}He+p subsystems. This region accommodates $3/2^-$ and $1/2^-$ resonance states of these subsystems with the Volkov potential. As seen in Fig. 10 (dashed lines), it yields a small contribution to the cross sections of the reactions ^{3}H(^{3}H,2n)^{4}He and ^{3}He(^{3}He,2p)^{4}He. This result contradicts the conclusions of Refs. [13,14]. In the two-cluster calculations of those references the $1/2^-$ state of the ^{4}He+N subsystem played a dominant role. We suspect this dominance to be due to the interplay of two factors: the weak coupling between incoming and outgoing channels, and the spin-orbit interaction.

In Fig. 11 we compare our results for the total proton yield [reaction ^{3}He(^{3}He,2p)^{4}He] to the experimental data from Ref. [25]. The latter were obtained for incident energy $E(^3\mathrm{He})=0.19$ MeV. One notices a qualitative agreement between the calculated and experimental data.

The cross sections, displayed in Figs. 10 and 11, were obtained with the maximal number of hyperspherical harmonics ($K\leqslant 10$). These figures should now be compared to Fig. 3, which displays some partial differential cross sections for a single *K* channel. The cross sections, displayed in Figs. 10 and 11, differ considerably from those in Figs. 3 and comparable ones, even for those hyperspherical harmonics which dominate the wave functions of the exit channel. An analysis of the cross section shows that the interference between the most dominant hyperspherical harmonics strongly influences the cross-section behavior. To support this statement we display the proton cross sections obtained with hypermomenta $K=0$, $K=2$, $K=4$ to those obtained with the full set of most important components $K_{\max}=4$ in Fig. 12. One observes a huge bump around 10 MeV which is entirely

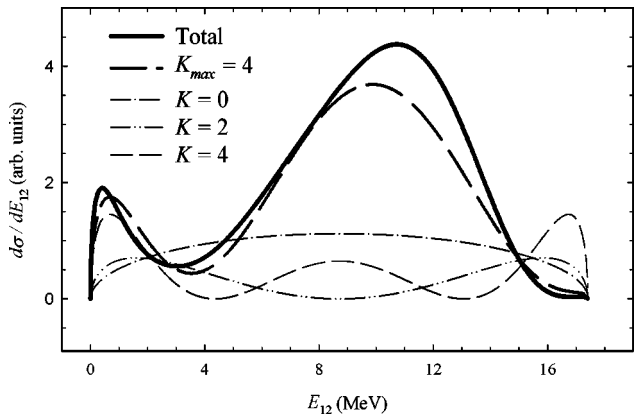

FIG. 12. Partial cross sections for the reaction ^{3}He(^{3}He,2p)^{4}He obtained for individual $K=0,2$, and 4 components, compared to the coupled calculation with $K_{\max}=4$ and the full calculations with $K_{\max}=10$.

due the interference of the different hyperspherical harmonic components. We also included the full calculation ($K_{\max}=10$) to indicate the rate of convergence for this cross section.

V. CONCLUSION

We have successfully considered the reactions ^{3}H(^{3}H,2n)^{4}He and ^{3}He(^{3}He,2p)^{4}He within the AM microscopic cluster model, which involves both two-cluster (^{3}He$+^3$He and ^{3}He$+^3$He) and three-cluster (^{4}He$+n+n$ and ^{4}He$+p+p$) configurations. A finite set of hyperspherical harmonics was used to describe the continuum of the three-cluster configurations. We demonstrated that the basis involved in our calculations was sufficiently large for convergent results. It was also demonstrated that only few hyperspherical harmonics dominate the reactions. Due to the weak coupling between two-cluster and three-cluster channels, the hyperspherical harmonics with the hypermomentum $K\geqslant 6$ lead to a negligible small contribution to the cross sections of the reactions ^{3}H(^{3}H,2n)^{4}He and ^{3}He(^{3}He,2p)^{4}He.

The theoretical results for the astrophysical S factor of the reactions are in a good agreement with the available experimental data. The analysis of the elastic and inelastic scattering parameters at low energy range ($0\leqslant E\leqslant 20$ keV) revealed no hidden resonance state within the current model accounting for the solar neutrino problem.

ACKNOWLEDGMENTS

This work was partially supported by an INTAS Grant (INTAS-93-755-extension). One of the authors (V. V.) gratefully acknowledges the University of Antwerp (RUCA) for support and the kind hospitality of the members of the research group ''Computational Quantum Physics'' of the Department of Mathematics and Computer Sciences, University of Antwerp, RUCA, Belgium.

[1] J. N. Bahcall, hep-ex/0002018.
[2] J. N. Bahcall, Nucl. Phys. **A631**, 29C (1998).
[3] W. C. Haxton, nucl-th/0004052.
[4] J. Bahcall and R. Davis, Jr., Publ. Astron. Soc. Pac. **112**, 429 (2000).
[5] W. C. Haxton and B. R. Holstein, Am. J. Phys. **68**, 15 (2000).
[6] E. G. Adelberger *et al.*, Rev. Mod. Phys. **70**, 1265 (1998).
[7] The LUNA Collaboration, M. Junker *et al.*, nucl-ex/9707003.
[8] The LUNA Collaboration, M. Junker *et al.*, Phys. Rev. C **57**, 2700 (1998).
[9] The LUNA Collaboration, R. Bonetti *et al.*, nucl-ex/9902004.
[10] The LUNA Collaboration, R. Bonetti *et al.*, Phys. Rev. Lett. **82**, 5205 (1999).
[11] V. S. Vasilevsky and I. Yu. Rybkin, Sov. J. Nucl. Phys. **50**, 411 (1989).
[12] K. Langanke, S. Typel, G. Bluge, and W. A. Fowler, Z. Phys. A **399**, 249 (1991).
[13] P. Descouvemont, Phys. Rev. C **50**, 2635 (1994).
[14] A. Csoto and K. Langanke, Nucl. Phys. **A646**, 387 (1999).
[15] V. S. Vasilevsky and F. Arickx, Phys. Rev. A **55**, 265 (1997).
[16] V. S. Vasilevsky, A. V. Nesterov, F. Arickx, and J. Broeckhove, Phys. Rev. C **63**, 034606 (2001).
[17] V. S. Vasilevsky, A. V. Nesterov, F. Arickx, and J. Broeckhove, Phys. Rev. C **63**, 034607 (2001).
[18] K. Varga and Y. Suzuki, Phys. Rev. C **52**, 2885 (1995).
[19] K. Varga, Y. Suzuki, and R. G. Lovas, Nucl. Phys. **A571**, 447 (1994).
[20] L. D. Faddeev and S. P. Merkuriev, *Quantum Scattering Theory for Several Particle Systems* (Kluwer, Dordrecht, 1993).
[21] A. B. Volkov, Nucl. Phys. **74**, 33 (1965).
[22] V. S. Vasilevsky, A. V. Nesterov, F. Arickx, and P. Van Leuven, Report No. ITP-96-3E, 1996 (unpublished).
[23] V. S. Vasilevsky, A. V. Nesterov, F. Arickx, and P. Van Leuven, Phys. At. Nucl. **60**, 343 (1997).
[24] Z. Papp, I. N. Filikhin, and S. L. Yakovlev, Few Body Syst., Suppl. **99**, 1 (1999).
[25] M. R. Dwarakanath and H. Winkler, Phys. Rev. C **4**, 1532 (1971).
[26] V. I. Serov, S. N. Abramovich, and L. A. Morkin, Sov. At. Energy **42**, 66 (1977).
[27] A. M. Govorov, L. Ka-Yeng, G. M. Osetinskii, V. I. Salatskii, and I. V. Sizov, Sov. Phys. JETP **15**, 266 (1962).
[28] R. E. Brown and N. Jarmie, Radiat. Eff. **84**, 45 (1986).
[29] H. M. Agnew, W. T. Leland, H. V. Argo, R. W. Crews, A. H. Hemmendinger, W. E. Scott, R. F. Taschek, Phys. Rev. **84**, 862 (1951).
[30] A. Krauss, H. W. Becker, H. P. Trautvetter, and C. Rolfs, Nucl. Phys. **A467**, 273 (1987).